NANO LETTERS

2005
Vol. 5, No. 11
2253−2256

Nanopore Tomography of a Laser Focus

Ulrich F. Keyser, Diego Krapf, Bernard N. Koeleman, Ralph M. M. Smeets, Nynke H. Dekker, and Cees Dekker*

Kavli Institute of Nanoscience, Delft University of Technology, Lorentzweg1, 2628 CJ Delft, The Netherlands

Received August 12, 2005; Revised Manuscript Received September 20, 2005

ABSTRACT

We demonstrate that the ionic current through a solid-state nanopore can be used to measure at single nanometer resolution the three-dimensional intensity profile of a laser directly in the focus of a microscope objective. We find a linear dependence of the ionic current on the incident laser power since the laser-induced heat increases the temperature locally in the solution. Our data show a temperature increase of up to 20 K in the center of the focus for a laser wavelength of 1064 nm. Measurements of the two-dimensional temperature profiles at different positions along the optical axis allow us to reconstruct the three-dimensional temperature profile of the laser focus, similar to tomography. Our new technique does not rely on the help of any optical elements and allows quantitative measurement of optical intensity or temperature distributions in aqueous environments with nanometer resolution.

It was shown recently that solid-state nanopores can be fabricated in thin membranes by a variety of different techniques.[1,2] The possibility to detect and to characterize biomolecules such as DNA using these nanopores was shown by a number of groups.[3−5] Here we propose and demonstrate a new application for solid-state nanopores, namely as local temperature sensor in an aqueous environment with nanometer resolution. We show that we can use this to reconstruct a tomographic image of the laser focus.

In the last 15 years, emerging single-molecule fluorescence techniques have boosted the further development of optical excitation schemes using total internal reflection[6] or second-harmonic generation.[7] The demand for an ever higher resolution has led to the development of new high numerical aperture (NA) objectives with NA > 1.6 (Olympus America Inc., Melville, NY). Although either power measurements[8,9] or probing the relative intensity distribution is possible with a spatial resolution of a hundred nanometers,[10−12] no technique exists that is able to provide nanometer precise spatial resolution and absolute power measurements at the same time. Knowledge of both the power and the shape of the laser focus is however essential for calculating the trapping potential in optical tweezers,[13] especially when optical constants of the whole optical system or its geometry are not well-known. This is of special importance for widely used single molecule tools such as laser tweezers[14] and confocal fluorescence microscopy.[15] The three-dimensional (3D) point spread function (PSF) and the absolute transmitted power measured directly in the focal spot of a microscope objective in liquids are necessary for a quantitative interpretation of the data, especially for reconstructing 3D microscopy images. With nanopore tomography, we introduce a new road for the quantitative characterization of optical elements far beyond the diffraction limit, achieving single nanometer resolution.

Figure 1a shows the essential components of the experimental configuration. The nanopores are mounted onto a home-built inverted microscope with a water immersion objective (UPLAPO, NA = 1.2, 60×, Olympus). A collimated infrared laser (λ = 1064 nm, 1.5 W, Crystalaser) overfills the back aperture of the objective and the nanopore position relative to the diffraction-limited focus is controlled by a closed-loop three-axis (x,y,z) piezoelectric stage (Physik Instrumente) with capacitive position feedback. An ionic-current amplifier (Axon Instruments) is used for measuring the linear current−voltage characteristic with a conductance between 20 and 150 nS, depending on the nanopore diameter.

The nanopores (typical diameter up to 10 nm) are fabricated in 20 nm thin low-stress silicon nitride (SiN) membranes. Fabrication starts with deposition of a sandwich layer on silicon using low-pressure chemical vapor deposition, yielding a 20 nm thin SiN layer, followed by 200 nm of TEOS SiO_2, and finally 500 nm of SiN (Figure 1b). A free-standing 700 nm thick membrane is obtained by etching the silicon in KOH.[16] In the center, this membrane is thinned over a circular region with a diameter of 5 μm by removal of the top two layers, using reactive ion etching and hydrofluoric acid. The top two layers serve two purposes: (1) they protect the 20 nm thin SiN layer during KOH etching of the Si and (2) they increase the mechanical stability of the membrane. In the 20 nm thin SiN membrane, nanopores are drilled in a transmission electron microscope (TEM) by

* Corresponding author. E-mail: dekker@mb.tn.tudelft.nl. Fax: +31 15 2781202.

10.1021/nl051597p CCC: $30.25
Published on Web 10/01/2005

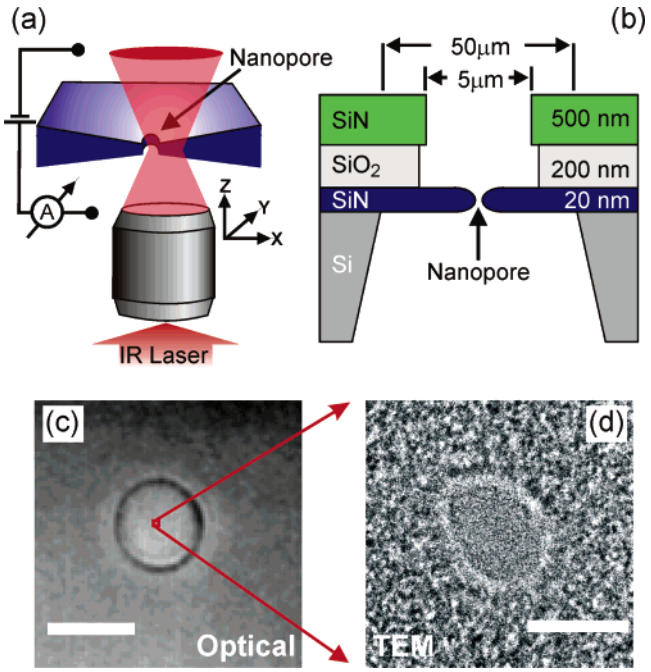

Figure 1. (a) Schematic image of the setup. The microscope objective focuses a laser into a diffraction-limited spot and the nanopore is scanned through the laser beam. The laser beam locally heats the liquid by absorption. (b) Side view of the layer structure of the completed samples with the nanopore drilled in the SiN membrane. (c) Optical top-view image of a SiN membrane with a diameter of 5 μm. The scale bar is 5 μm long. (d) TEM image of a typical nanopore with a diameter of 4 nm. The scale bar is 4 nm, 1250 times smaller than that in part c.

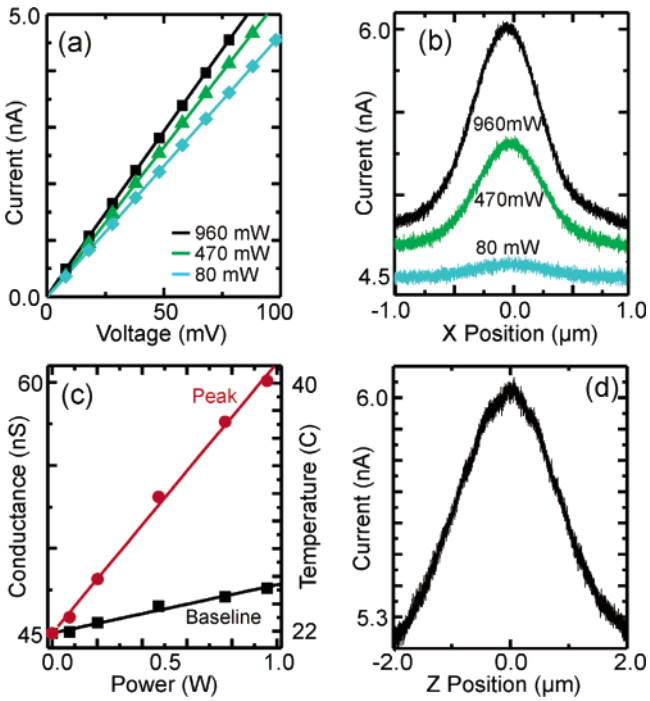

Figure 2. (a) Ionic current through a nanopore (diameter 5 nm) as a function of voltage for three different laser powers. Points represent the experimental data; the lines are linear fits. The colors correspond to the same powers as used in part b. (b) Current through the same nanopore as a function of *x*-position through the laser focus for three different laser powers. (c) Conductance as a function of the laser power extracted from data such as in part b. The red data represent the peak conductance and the black values the baseline. The lines are linear fits. The right axis shows the corresponding temperature values. (d) Current through the nanopore as a function of *z*-position at a laser power of 960 mW.

tightly focusing the electron beam on the SiN membrane. The focused electron beam leads to the formation of small holes by sputtering atoms from the SiN layer.[2] Figure 1c shows an optical microscopy image of the membrane in solution obtained with a CCD camera. Figure 1d shows a TEM image of a typical nanopore with a diameter of ~4 nm, which is 1/1000 of the membrane diameter. A single pixel in Figure 1c covers 100 times the area of the TEM image in Figure 1d.

The nanopores were mounted into our custom-made inverted microscope using a microfluidic PDMS flow cell designed with an optical window. Both sides of the nanopores were flushed with a 1 M KCl salt solution with 10 mM Tris-HCl buffer at pH = 8.0. Detection of the ionic current is achieved with platinum wires that are immersed in a separate compartment containing 1 M KCl together with 1 mM potassium ferri- and ferrocyanide and connected via agarose-gel salt bridges to the flow cell. These electrodes prevent measuring parasitic photocurrents typical for light-sensitive Ag/AgCl reference electrodes.[17,18] A 30 s cleaning of the nanopore in an oxygen plasma prior to use facilitates its wetting.

We scan the nanopore through the laser focus and simultaneously record the ionic current flowing through the nanopore. Figure 2a shows the ionic current as a function of applied voltage in a 5 nm nanopore for three incident laser powers, while the laser was focused directly on the nanopore. The incident laser power was measured in front of the back aperture of the objective with a commercial power meter. The points show the experimental data, and the lines are linear fits. Clearly, the nanopore conductance is linear and depends on the incident laser power.

In Figure 2b the current through the pore is shown at a constant voltage of 100 mV as a function of the *x*-position when we scan the nanopore through the laser focus. The figure shows data for three laser powers. In our experiments we typically use a slow scanning speed of 1 μm/s to ensure that thermal equilibrium is reached at every position.[19] We observe that with increasing laser power the peak gets higher and simultaneously the background conductance increases due to heating of the entire flow cell.

From these data, we calculate the local temperature by using the linear temperature dependence of the conductivity of KCl,[20] and assuming a constant factor for the nanopore geometry. As the reference point we measure the nanopore conductance at 21 °C in our temperature-stabilized laboratory prior to turning on the laser, and scale this value to the bulk conductivity of 1 M KCl. From the conductance enhancement we then obtain the local temperature *T*. This method is justified as we find both a linear dependence of conductance for both the bulk solution temperature and the local temperature in the laser focus (Figure 2c). The temperature increase in the focus can reach up to 20 K, which fits very well with values previously observed in optical traps.[19] In

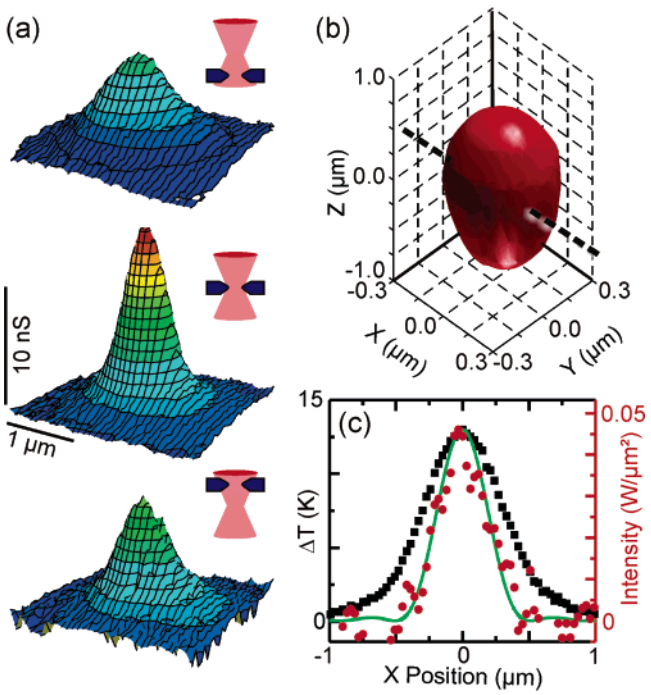

Figure 3. (a) Topographic maps of the conductance through a nanopore (diameter 5 nm) at different, constant *z*-positions $z = +1\ \mu$m (top), $z = 0\ \mu$m (center), and $z = -1\ \mu$m (bottom), with an incident laser power of 960 mW. (b) Three-dimensional surface reconstruction from a set of nine such scans. We show the surface for 11 nS. (c) Temperature difference (black) and numerically derived laser intensity (red) as a function of position through the center of the focus marked by the dashed line in part b. The green line is not a fit but the intensity as calculated for a perfect lens and scaled to the peak value.

Figure 2d we show the current through the nanopore as a function of the laser focus *z*-position. As expected, the peak has a larger full width at half-maximum because it is measured in the direction of the laser beam.

We now obtain the three-dimensional shape of the laser focus by scanning several two-dimensional current maps at different positions along the optical axis. With these data, we reconstruct a three-dimensional image of the laser focus, analogous to tomography. In Figure 3a, three typical maps of the nanopore conductance $G(x,y,z)$ are shown as the nanopore scans through the laser focus in a x,y-plane at different z-positions. The nanopore maps out a peak in G that broadens and decreases as we move the nanopore out of focus, as shown in Figure 3a top and bottom. Figure 3b shows the reconstructed surface of constant $\Delta G = 11$ nS that was obtained from a series of these scans. Since $G(T)$ depends linearly on T, the resulting ellipsoid represents an isothermal surface.

Quantitatively, the change of the conductance can be explained as follows. The laser power will be absorbed in the solution near the focus, which changes the local temperature T, and thus influences the conductance $G(T)$ of the nanopore. We neglect any contributions from the SiN membranes because no significant amount of the laser power is absorbed in the membrane and the thermal conductivity of the SiN will only change our values by a minute amount. In steady state, the temperature profile is directly linked to the laser intensity I via the differential equation $\kappa\nabla^2 T + \alpha I = 0$ with the absorption coefficient $\alpha(H_2O) = 0.12\ \text{cm}^{-1}$ and the thermal conductivity $\kappa(H_2O) = 0.6\ \text{W m}^{-1}\ \text{K}^{-1}$. Upon extracting the temperature from our nanopore measurements as described above, we are able to directly calculate the laser intensity by numerically computing $I = -(\kappa/\alpha)\nabla^2 T$. In Figure 3c we show the temperature change ΔT and the numerically obtained laser intensity as a function of position from the center of the focus. The full width at half-maximum of the latter is 550 ± 20 nm, which fits excellently with the diffraction limit of 541 nm for an aberration-free lens. The green line in Figure 3c is the calculated intensity distribution for a diffraction-limited lens with the same numerical aperture. By integrating I over the area, we deduce an overall laser power of 500 ± 80 mW, which yields a transmission of 52 ± 8% in good agreement with the expected value of 65% taking into account losses in the optical path to the nanopore such as reflections at the cover glass surface.

In conclusion, we report a completely new, nanopore-based technique to quantitatively measure with single nanometer precision the three-dimensional intensity distribution of light in aqueous environment. We demonstrate this by measuring spatially resolved the absolute intensity of a laser beam focused by a microscope objective with high numerical aperture in a salt solution. From the temperature profiles, we are able to compute the absolute transmitted power. Knowledge of both the transmitted power and the exact shape of the beam is very important for single-molecule techniques such as optical tweezers or fluorescence correlation spectroscopy. By tuning the absorption properties of the solution, it may be possible to adjust the sensitivity to different wavelengths and lower powers. We have demonstrated that our solid-state nanopore-based technique can detect temperature profiles with nanometer precision. Future work will determine the applicability of this method for measuring temperature close to nanostructures where heat dissipation can be more rapid, thus requiring detection of smaller temperature changes.

Acknowledgment. We thank Derek Stein and Bernadette Quinn for stimulating discussions and the group of Henny Zandbergen for providing access to the TEM. Financial support by FOM and NWO is gratefully acknowledged.

References

(1) Li, J.; Stein, D.; McMullan, C.; Branton, D.; Aziz, M.; Golovchenko, J. *Nature* **2001**, *412*, 166−169.
(2) Storm, A.; Chen, J.; Ling, X.; Zandbergen, H.; Dekker, C. *Nat. Mater.* **2003**, *2*, 537−540.
(3) Heng, J.; Ho, C.; Kim, T.; Timp, R.; Aksimentiev, A.; Grinkova, Y.; Sligar, S.; Schulten, K.; Timp, G. *Biophys. J.* **2004**, *87*, 2905−2911.
(4) Li, J.; Gershow, M.; Stein, D.; Brandin, E.; Golovchenko, J. *Nat. Mater.* **2003**, *2*, 611−615.
(5) Storm, A.; Storm, C.; Chen, J.; Zandbergen, H.; Joanny, J.; Dekker, C. *Nano Lett.* **2005**, *5*, 1193−1197.
(6) Macklin, J.; Trautman, J.; Harris, T.; Brus, L. *Science* **1996**, *272*, 255−258.
(7) Bouhelier, A.; Beversluis, M.; Hartschuh, A.; Novotny, L. *Phys. Rev. Lett.* **2003**, *90*, 013903.
(8) Neuman, K.; Chadd, E.; Liou, G.; Bergman, K.; Block, S. *Biophys. J.* **1999**, *77*, 2856−2863.

(9) Viana, N.; Mesquita, O.; Mazolli, A. *Appl. Phys. Lett.* **2002**, *81*, 1765−1767.
(10) Jia, B.; Gan, X.; Gu, M. *Appl. Phys. Lett.* **2005**, *86*, 131110.
(11) Rhodes, S.; Barty, A.; Roberts, A.; Nugent, K. *Opt. Commun.* **1998**, *145*, 9−14.
(12) Rhodes, S.; Nugent, K.; Roberts, A. *J. Opt. Soc. Am. A* **2002**, *19*, 1689−1693.
(13) Neto, P.; Nussenzveig, H. *Europhys. Lett.* **2000**, *50*, 702−708.
(14) Bustamante, C.; Bryant, Z.; Smith, S. *Nature* **2003**, *421*, 423−427.
(15) Hess, S.; Huang, S.; Heikal, A.; Webb, W. *Biochemistry* **2002**, *41*, 697−705.
(16) Sze, S. M. *Semiconductor Devices, Physics and Technology*, 2nd ed.; Wiley: New York, 2002; p 428.
(17) Caldwell, W.; Smith, L. *Phys. Rev.* **1948**, *74*, 1207−1207.
(18) Banks, F. *Phys. Rev.* **1948**, *74*, 1207−1208.
(19) Peterman, E.; Gittes, F.; Schmidt, C. *Biophys. J* **2003**, *84*, 1308−1316.
(20) Pratt, K.; Koch, W.; Wu, Y.; Berezansky, P. *Pure Appl. Chem.* **2001**, *73*, 1783−1793.

NL051597P